Acylating Capacity of the Phosphotungstic Wells−Dawson Heteropoly Acid: Intermediate Reactive Species

Sebastián E. Collins,[†] Silvana R. Matkovic,[‡] Adrian L. Bonivardi,[†] and Laura E. Briand*[,‡]

Centro de Investigación y Desarrollo en Ciencias Aplicadas-Dr. Jorge J. Ronco, Universidad Nacional de La Plata, CONICET, CCT La Plata, Calle 47 N 257, B1900AJK La Plata, Buenos Aires, Argentina, and Instituto de Desarrollo Tecnológico para la Industria Química INTEC, Universidad Nacional del Litoral, CONICET, Güemes 3450, 3000 Santa Fé, Argentina

Received: August 24, 2010; Revised Manuscript Received: November 25, 2010

The mechanism of adsorption and decomposition of acetic anhydride over phosphotungstic Wells−Dawson heteropoly acid (HPA) was investigated through infrared spectroscopy with especially dedicated *in situ* cells. Both gaseous and liquid acetic anhydride dissociatively chemisorbs on the heteropoly acid, producing the intermediate acyl CH_3CO^+ species, adsorbed acetate species, and acetic acid. The former is known as the key intermediate species in the Friedel−Crafts acylation reaction. Moreover, the consumption of the Brønsted acid sites observed during the adsorption and decomposition of acetic anhydride over the HPA indicates that those sites are the active ones of the genesis of the acyl intermediate species. Surface acetate species and acetic acid strongly adsorb on the active acid sites deactivating the heteropoly acid.

1. Introduction

Typically, a Friedel−Crafts acylation process is an electrophilic substitution reaction where an acyl halide (usually, RCOCl) activates over an acid catalyst through the formation of an intermediate reactive carbocation ($RC{\equiv}O^+$) species. This acylium ion is an electrophilic species that further reacts with an aromatic substrate (nucleophilic species) given a ketone product.

This process that was initially reported in 1877 experimented numerous modifications and advances in order to achieve a greener pathway to obtain valuable aromatic ketones.[1] Table 1 summarizes the applications of the Friedel−Crafts acylation (focusing on the past 10 years of literature), catalytic materials, active surface sites, and substances that have been used as acylating reagents and indicates if the reaction was carried out in the liquid or gas phase and homogeneous or heterogeneous conditions.

The literature shows three main groups of substances that have been used as acid catalysts in the Friedel−Crafts acylation process: liquid mineral acids and acyl halides, zeolites and resins, and, more recently, heteropoly compounds.

The first group comprises inorganic acids (e.g., HF) and solid acid materials with Lewis acid sites (e.g., $AlCl_3$, $TiCl_4$) used in homogeneous media, that is, dissolved in the liquid reaction media.[2−4] These systems catalyze the formation of the acyl intermediate through the complexation of the halide of the acylating agent. Although these materials are called "catalysts", they act as "reagents", since they are used in stoichiometric amounts and are not reusable.

A second group of materials involves zeolites and resins such as HZSM5, beta zeolite, H-mordenite, Nafion, and Amberlyst,[5−8] which possess mainly Brønsted acid sites and a certain contribution of Lewis sites. These systems are not soluble in the reaction media (liquid/gaseous reagents and solid catalyst) and are suitable to activate other acyl donors rather than harmful acyl halides. These are important improvements toward an environmentally friendly Friedel−Crafts process, since the catalyst is easily separated from the reaction media, might be reusable, and the production of dangerous gases (e.g., HCl from the decomposition of the acyl halide) is avoided.

More recently, many investigations devoted to Friedel−Crafts acylation catalyzed with heteropoly acids (HPAs) and salts are found in the literature.[9−14] These materials possess strong Brønsted acid sites even though the salts combine both large monovalent cations (e.g., K^+, Cs^+, Rb^+, NH_4^+) and protons as counterions. This combination allows obtaining water insoluble, high surface area materials along with a controlled porous structure.[15] Heteropoly compounds with the Keggin structure catalyze the acylation of a variety of aromatic compounds with acyl chlorides and anhydrides, as can be seen in Table 1. However, the affinity of HPAs toward polar oxygenates leads to the irreversible adsorption of byproduct and/or the acyl donor on the acid sites, causing its deactivation. The investigation of Anderson et al. addressed the causes of the deactivation of supported phosphotungstic Keggin acid during the acylation of anisole with acetic anhydride.[16] Their investigation suggested that the observed deactivation is due to the strong adsorption of the product (*p*-methoxyacetophenone), and other hydrocarbonaceous residues derived from the polyacetylation of anisole and condensation byproduct, on the catalyst.

To the knowledge of the authors, no investigations on other heteropoly compounds rather than of the Keggin-type one have been reported in the literature.

The Friedel−Crafts acylation of isobutylbenzene with acetic anhydride has been chosen in this work as a probe reaction in order to establish if the phosphotungstic Wells−Dawson heteropoly acid is able to activate the acyl donor. It is desirable that the acylation of isobutylbenzene generates *p*-isobutylacetophenone which is an intermediate in the production of ibuprofen.[17] Nowadays, this step of the industrial production of ibuprofen is catalyzed with liquid fluorhydric acid (see Table

* Corresponding author. E-mail: briand@quimica.unlp.edu.ar. Phone: 54 221 4 211353/210711.
[†] Universidad Nacional del Litoral.
[‡] Universidad Nacional de La Plata.

10.1021/jp108031h
Published on Web 01/04/2011

TABLE 1: Summary of the Most Relevant Investigations of Friedel−Crafts Processes: Reagent That Is Acylated, Catalytic Material, Acylating Reagent, Active Surface Sites Characteristics, Gas or Liquid Phase (the Solvent Is indicated) Reaction Media, and Homogeneous or Heterogeneous Phase

reagent	catalyst	acylating reagent	active surface site	reaction medium	ref
alkylbenzene	$AlCl_3$	acyl chloride	Lewis acid sites	liquid (CH_2Cl_2), homogeneous	2
isobutylbenzene	HF	acetic anhydride, acetyl fluoride		liquid, homogeneneous	3
anisole	indium complexes: $InCl_3$, $In(OTf)_3$ with $LiClO_4$ as additive	isopropenyl acetate	Lewis acid sites	liquid (nitrometane) homogeneous	4
toluene	sulfated oxides (ZrO_2, SnO_2, TiO_2, HfO_2, Fe_2O_3) and supported WO_x species	benzoic anhydride, benzoyl chloride, acetic anhydride	Lewis acid sites	liquid (tridecane) heterogeneous	5
toluene	zeolites: HZSM5, H-mordenite	acetic anhydride, acyl chl., acetic ac.	Brønsted acid sites	gas phase	6
anisole, veratrole, isobutylbenzene, heterocycle compounds	beta zeolite	acetic anhydride	Brønsted + Lewis acid sites	liquid ($C_2H_4Cl_2$) heterogeneous	7
phenol	Al-MCM-41, zeolites HY, HZSM-5, HBeta	acetic acid	Brønsted + Lewis acid sites	gas phase	8
benzene	Keggin heteropoly salts: $K_{2.5}H_{0.5}PW_{12}O_{40}$; $Rb_{2.5}H_{0.5}PW_{12}O_{40}$; $Cs_{2.5}H_{0.5}PW_{12}O_{40}$; $Cs_{2.5}H_{0.5}PMo_{12}O_{40}$; $K_2H_2SiW_{12}O_{40}$; $(NH_4)_2HPW_{12}O_{40}$	benzoic anhydride, benzoyl chloride	Brønsted acid sites	liquid, heterogeneous	9
p-xylene					
anisole	$H_3PW_{12}O_{40}$; $H_3PMo_{12}O_{40}$; $H_3PW_{12}O_{40}/SiO_2$	acetic anhydride	Brønsted acid sites	liquid, heterogeneous	10
veratrole [$C_6H_4(OCH_3)_2$]	$H_3PW_{12}O_{40}$/hexag. mesoporous SiO_2	acetic anhydride	Brønsted acid sites	liquid ($C_2H_4Cl_2$) heterogeneous	11
anisole	$H_3PW_{12}O_{40}/SiO_2$	acetic anhydride	Brønsted acid sites	liquid (CH_3Cl, $C_2H_4Cl_2$, toluene) heterogeneous	12
benzene	$Cs_{2.5}H_{0.5}PW_{12}O_{40}$	benzoic anhydride	Brønsted acid sites	liquid (*n*-tetradecane) heterogeneous	13
thioanisole	$K_{2.5}H_{0.5}PW_{12}O_{40}$/clay acid resins	acetic anhydride	Brønsted + Lewis, only Brønsted sites for resins	liquid ($C_2H_4Cl_2$) heterogeneous	14

1, ref 3), which is quite a dangerous, nonenvironmentally friendly chemical and requires costly noncorrosive facilities.[17−19] Therefore, the replacement of the inorganic liquid acid by a solid acid such as the heteropoly acid studied here might represent an important contribution toward the development of an ecofriendly technology.

The present work provides evidence of the surface intermediate species (both reactive and nonreactive) formed over the Wells−Dawson phosphotungstic heteropoly acid exposed to an acylating agent such as acetic anhydride.

2. Experimental Section

2.1. Materials and Reaction Procedure. The phosphotungstic Wells−Dawson heteropoly acid $H_6P_2W_{18}O_{62}\cdot xH_2O$ was synthesized through ion exchange of the phosphotungstic $(NH_4)_6P_2W_{18}O_{62}\cdot 13H_2O$ salt with an ion-exchange resin as reported previously.[20] This acid was dispersed over TiO_2 (Aeroxide P-18 Evonik Ind., 46.8 ± 0.1 m^2/g), ZrO_2 (fumed Evonik Ind., 39.4± 0.4 m^2/g), and SiO_2 (Cab-O-Sil) (328.9 ± 0.8 m^2/g) through conventional incipient wetness impregnation, further dried overnight at 373 K, and calcined at 573 K for 4 h. The synthesized materials for the infrared study of the acyl intermediate were 14% HPA/ZrO_2, 15% HPA/TiO_2, and 9% HPA/SiO_2. Although the amount of HPA supported on zirconia and titania oxide supports corresponds to the hypothetical monolayer coverage of the phosphotungstic heteropolyanion $P_2W_{18}O_{62}{}^{6-}$, both *in situ* Raman and infrared analyses demonstrated that the heteropoly acid is in the crystalline form and not dispersed as a monolayer film. These findings are not further discussed in the present paper, since they are not the objective of the present investigation.

Additionally, for the study of the acylation reaction of isobutylbenzene, 33−66% HPA/SiO_2 was also used. Other acidic materials such as tungsten oxide species supported over mesoporous zirconium dioxide nanoparticles 30% WO_3/ZrO_2 (provided by the Operando Molecular Spectroscopy and Catalysis Laboratory at Lehigh University, PA), commercial Dowex HCR-W2 ion-exchange resin (Sigma Aldrich, 2.4 mequiv/g of exchangeable protons), and HZSM5 zeolite (Zeolyst International) were also evaluated as catalytic materials.

Typically, the reaction was performed by adding acetic anhydride (J. T. Baker 99%) to a mixture of the catalytic material and isobutylbenzene (Aldrich 99%) in a three-necked bottom flask equipped with a condenser system. The resultant suspension was heated while stirring at the desired temperature in an oil bath equipped with an automatic temperature control system. Samples of the reaction mixture were periodically withdrawn (from 30 min up to 24 h of reaction) with a filtering syringe (Sartolon Polyamid, 0.45 μm). The samples were analyzed through HPLC using a C18 column (Supelcosil) with a UV detector (ChromTech UV230$^+$) operated at 254 nm. The mobile phase (methanol:H_2O (80:20 v/v)) was operated at a flow rate of 0.7 mL/min. All samples were run in triplicate. Additionally, the identity of the products was further confirmed with GC-MS analysis (Perkin-Elmer Q-Mass 910 mass spectrometer with an Autosystem Gas Chromatograph).

2.2. In Situ Infrared Investigation of Surface Intermediate Species. ***2.2.1. Adsorption-Reaction of Substances in the Gas Phase.*** The adsorption of acetic anhydride on supported phosphotungstic Wells−Dawson heteropoly acid and the bare oxide supports (TiO_2, ZrO_2, and SiO_2) was investigated through *in situ* transmission infrared spectroscopy on self-supported wafers (30 mg) pressed at 5 t/cm^2 (diameter = 13 mm). The wafers were placed into a Pyrex IR cell fitted with water-cooled NaCl windows, which was attached to a conventional high vacuum system (base pressure = 1.33×10^{-4} Pa), equipped with a manifold for gas flow operation. Before the adsorption experiments, each sample was calcined *in situ* at 473 K for 30 min and allowed to cool up to 303 K under a pure helium flow (60 sccm) to allow reference IR spectra of the "clean wafer" to

TABLE 2: Summary of the Various Acidic Materials and Reaction Conditions Investigated in the Friedel−Crafts Acylation of Isobutylbenzene with Acetic Anhydride[a]

materials	pretreatment	reaction temperature (K)	acidic material and reactant ratio[b] (g/mol)	IBB:AA mol ratio	added cosolvents	products detected	deactivation
bulk $H_6P_2W_{18}O_{62}$	fully hydrated, no-pretreatment	323	4.5	3:1 (excess IBB)	none	IBA phenone	yes
		353	23.7	0.3:1 (excess AA)			
	dehydrated at 673 K		31.7				
			49.0				
33% HPA/SiO_2		333	0.2	2:1 (excess IBB)	none	IBA phenone	yes
60% HPA/SiO_2	calcined at 573 K	353	0.5				
15% HPA/TiO_2		368	1.0				
14% HPA/ZrO_2			2.0				
9% HPA/SiO_2	calcined at 573 K	353	12.0	2:1 (excess IBB)	acetonitrile	IBA phenone	yes
45% HPA/SiO_2				1:3 (IBB+AA): solvent mol ratio	toluene		
					tetrahydrofuran		
30% WO_3/ZrO_2	calcined at 773 K	353	1.0	2:1 (excess IBB)	none	nonreactive	nonreactive
		373					
Dowex resin	none	333	24.0	2:1 (excess IBB)	none	nonreactive	nonreactive
		353	74.0		water		
		368					
HZSM5 zeolite	none	353	3.4	0.3:1 (excess AA)	none	nonreactive	nonreactive
		413	17.1				

[a] HPA, phosphotungstic Wells−Dawson heteropoly acid ($H_6P_2W_{18}O_{62}$); IBB, isobutylbenzene; AA, acetic anhydride; IBA phenone, *p*-isobutylacetophenone. [b] The ratio between the amount of material and reactants corresponds to the weight of catalyst in grams per mol of IBB and AA.

be taken at different temperatures. IR spectra were taken every 50 K along the cooling process.

The gas used in this study was high purity grade He (AGA UHP 99.999%) and was further purified through a molecular sieve (3 Å) and MnO/Al_2O_3 traps to remove water and oxygen impurities, respectively.

Acetic anhydride (J. T. Baker, 99%) was purified by a series of freeze−thaw cycles, under vacuum, to remove dissolved gases and was stored at room temperature (RT) in a glass bulb attached to the manifold. Then, gaseous acetic anhydride was allowed into a small section of the manifold (which featured a sampling loop) and, then, was swept from the loop by flowing He (60 sccm) to the IR cell at RT to avoid decomposition. After acetic acid adsorption onto the wafer, the cell was purged for 30 min under He flow (60 sccm). The evolution of the adsorption-reaction process was followed by heating the IR cell from RT to 473 at 10 K min^{-1} still flowing He (60 sccm). Along the temperature ramp, transmission infrared spectra were recorded at 323, 368, 423, and 473 K.

A Nicolet Magna 550 FTIR spectrometer with a DLATGS detector was used to acquire the spectra (4 cm^{-1} resolution, 100 scans). The overlapping bands, along with the measurement of peak areas, were solved using a special peak fitting module of Origin 4.0 software. Background correction of the spectra was achieved by subtracting the spectra of the pretreated cleaned wafer at each temperature.

2.2.2. Adsorption-Reaction of Substances in the Liquid Phase. The adsorption of acetic anhydride and acetic acid on oxide supported phosphotungstic Wells−Dawson heteropoly acid was also studied through *in situ* transmission infrared spectroscopy in the liquid medium. These investigations were performed in a homemade *in situ* liquid flow-through cell built with two complementary Teflon bodies and fitted with CaF_2 windows. A Teflon ring allows an inner space (ranging between 50 and 500 μm) to locate a sample wafer between the windows (wafer preparation was previously detailed). One of the CaF_2 windows has two drilled orifices to allow the inlet and outlet of the liquid flow through the cell. Typically, carbon tetrachloride (Merck, 99%) was used as a liquid carrier flowing at 1 mL min^{-1} by means of a very low pulsation and high repeatability peristaltic pump (Ismatec ICP 4). The reactants were used in a 1:10 (substance: CCl_4) molar ratio in the experiments, which will be described in the following sections.

The samples were calcined *in situ* under flowing Ar (50 sccm) at 373 K for 60 min before the adsorption of the acylating substances. The evolution of the adsorption-reaction process was followed by flowing the reactants through the cell, which were heated in a water bath from RT to 417 K. Along the temperature stepped ramp, transmission infrared spectra were recorded at 307, 315, and 417 K.

2.2.3. Isotopic Exchange with D_2O. The H−D isotopic exchange of water molecules and heteropoly acid hydroxyl groups with deuterium oxide (D > 99%) was also performed in the *in situ* liquid flow-through cell described above. The sample was contacted with D_2O at 348 K for 10 min, and then purged *in situ* under flowing Ar (60 sccm) at the same temperature for 30 min. The sample was cooled down to RT before being exposed to the liquid carrier CCl_4.

3. Results

3.1. Friedel−Crafts Acylation of Isobutylbenzene with Acetic Anhydride Catalyzed with Acidic Materials. The acylation of isobutylbenzene with acetic anhydride over bulk and oxide supported HPA was investigated in the liquid phase at various temperatures, hydrated and dehydrated, various ratios of reactants, excess of either the acylating agent or isobutylbenzene, with and without cosolvents, and over extended periods of time (up to 24 h of reaction). Moreover, not only the phosphotungstic Wells−Dawson heteropoly acid was tested but other materials that possess well-known acid properties were also assayed. Table 2 summarizes the variety of materials and the reaction conditions that were investigated in order to achieve the synthesis of *p*-isobutylacetophenone through the acylation of isobutylbenzene.

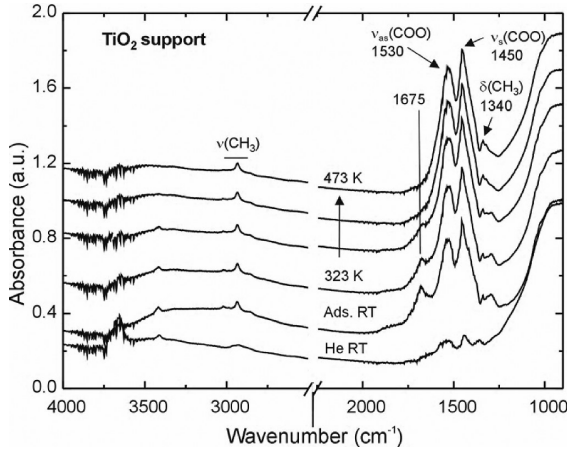

Figure 1. Infrared spectra obtained under *in situ* conditions of titania support after calcination at 473 K and during the adsorption of gaseous acetic anhydride from RT to 473 K (Ads., adsorption).

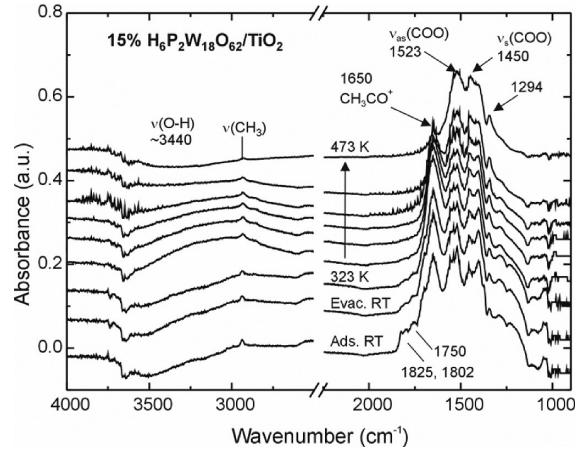

Figure 2. Infrared spectra obtained under *in situ* conditions during the adsorption of gaseous acetic anhydride over 15% $H_6P_2W_{18}O_{62}/TiO_2$ (after calcination at 473 K) from RT to 473 K (Ads., adsorption; Evac., evacuated).

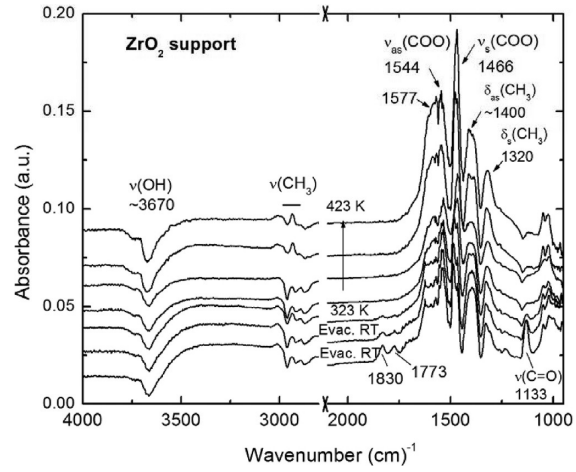

Figure 3. Infrared spectra obtained under *in situ* conditions during the adsorption of gaseous acetic anhydride over zirconia support (after calcination at 473 K) from RT to 423 K (Evac., evacuated).

The results demonstrated that both bulk and supported HPA regardless of the loading and the nature of the oxide support (SiO_2, TiO_2, ZrO_2), catalyze the acylation of isobutylbenzene toward *p*-isobutylacetophenone at temperatures as low as 323 K. However, those materials deactivate at the very beginning of the reaction, leading to a negligible conversion of isobutylbenzene. The addition of a cosolvent such as toluene, acetonitrile, and tetrahydrofuran, which are regularly used in organic synthesis, did not recover the activity of the HPA.

Other acidic materials such as monolayer tungsten oxide species supported over mesoporous ZrO_2 nanoparticles, commercial Dowex resin, and HZSM5 zeolite were also tested in the Friedel−Crafts acylation of isobutylbenzene with acetic anhydride. Surprisingly, none of those materials possesses the capacity of catalyzing the acylation of isobutylbenzene, since no products were observed.

There is no doubt that the capability of the HPA of catalyzing the selective acylation of isobutylbenzene is a valuable observation considering that, to the knowledge of the authors, the literature only reports the use of beta-zeolite as an active material in that reaction. However, the deactivation of the heteropoly acid is a serious drawback that deserves an exhaustive investigation in order to be able to molecularly redesign that material for a technological application, which is beyond the aim of this work.

3.2. In Situ Investigation of the Surface Interaction of Gaseous Acetic Anhydride with Supported Wells−Dawson Phosphotungstic Heteropoly Acid. The interactions of gaseous acetic anhydride with supported phosphotungstic Wells−Dawson acid and pure oxide supports were investigated through *in situ* infrared spectroscopy. The investigations were performed over the supported HPA, since the attempts to make a wafer with the bulk HPA have not been successful. Moreover, the interaction of acetic anhydride with pure TiO_2, ZrO_2, and SiO_2 oxide supports was investigated in order to fully understand the chemisorption-reaction process.

Figures 1 and 2 show the infrared spectra of acetic anhydride adsorbed on the bare TiO_2 support and on the phosphotungstic Wells−Dawson acid supported on TiO_2, respectively. It is important to notice that the contribution of the solid has been subtracted in each case from the spectra corresponding to the adsorption of acetic anhydride on pure oxide supports and the supported heteropolyacid discussed along this section. Then, the spectra show signals of the (surface) adsorbed species.

The absence of the characteristic couple of signals due to the carbonyl stretching at 1831−1809 and 1760 cm^{-1} of liquid acetic anhydride demonstrates that the anhydride is not molecularly adsorbed on the supported HPA or the oxide support surface.[21,22]

The anhydride adsorption on TiO_2 develops intense signals ascribed to surface acetate species (1450 and 1530 cm^{-1}) that remain adsorbed even at high temperature.[23−25] The supported heteropoly acid shows the presence of acetate species along with a couple of new signals at 1650 (observed at 1675 cm^{-1} on the titania support) and 1294 cm^{-1} that might be attributed to an acetyl intermediate, as will be discussed in the following sections. The Brønsted acid sites of the HPA (at ∼3440 cm^{-1}) that remain after calcination at 473 K were consumed during the adsorption process.

Figures 3 and 4 show the infrared spectra of acetic anhydride adsorbed on the bare ZrO_2 support and the phosphotungstic Wells−Dawson acid supported on ZrO_2, respectively. The spectra of the ZrO_2 after adsorption of acetic anhydride at RT followed by evacuation show the characteristic signals of molecular acetic anhydride at 1830 and 1773 cm^{-1} along with the surface adsorbed acetate species (1544 and 1466 cm^{-1}). Similarly, as observed on TiO_2, the acetate species dominate the spectra upon raising the temperature and remain strongly adsorbed even at 423 K. The adsorption of acetic anhydride over ZrO_2 supported HPA develops surface adsorbed acetate species along with a new signal at 1665 cm^{-1} (this last one

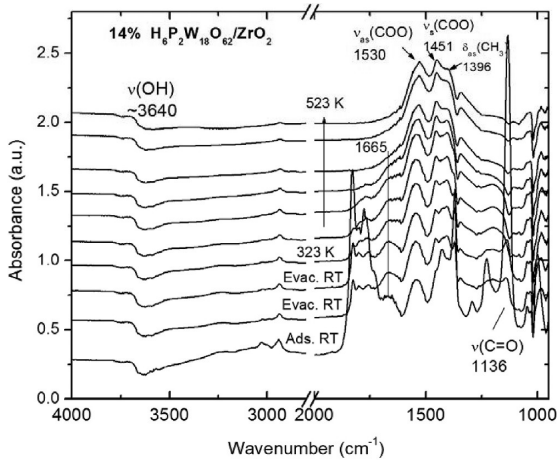

Figure 4. Infrared spectra obtained under *in situ* conditions during the adsorption of gaseous acetic anhydride over 14% $H_6P_2W_{18}O_{62}/ZrO_2$ (after calcination at 473 K) from RT to 523 K (Ads., adsorption; Evac., evacuated).

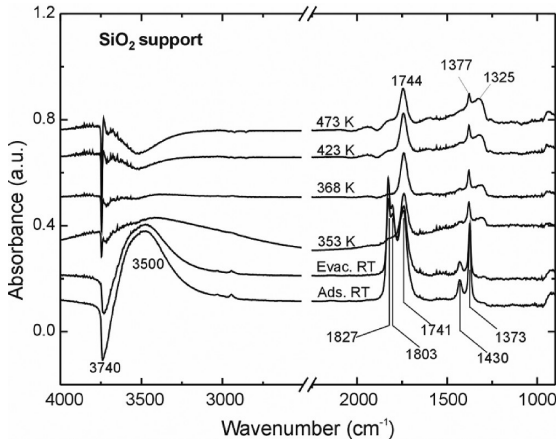

Figure 5. Infrared spectra obtained under *in situ* conditions of silica support (after calcination at 473 K) and during the adsorption of gaseous acetic anhydride from RT to 473 K (Ads., adsorption; Evac., evacuated).

vanishes above 423 K). This low intensity signal might be an evidence of the formation of acyl species on the HPA as discussed above.

Silica presents a completely different behavior after being in contact with the anhydride, as can be observed in Figure 5. The anhydride was molecularly adsorbed on the silica at RT, as shown by the characteristic infrared bands at 1827, 1803, 1741, 1430, and 1373 cm^{-1}.[22] Upon heating to 353 K, those bands vanished and a set of signals showed up at 1744, 1377, and 1325 cm^{-1}, which can be assigned to silyl ester surface species and/or acid molecules strongly adsorbed on the terminal silanol groups,[22,23] whose stretching mode in turn shifted from 3740 (negative peak) to ca. 3500 cm^{-1}.[16,21] Also, the broad band around 3500 cm^{-1} could contain a contribution from the ν(OH) of molecularly adsorbed acetic acid. Notice that acetic acid/silyl ester species remains adsorbed even upon heating up to 473 K.

When acetic anhydride was put in contact with the supported phosphotungstic Wells−Dawson acid on silica, 9% $H_6P_2W_{18}O_{62}/SiO_2$, strong signals due to adsorbed acetic acid bonded to the terminal silanol groups were immediately observed at RT (see Figure 6). Again, a negative signal at 3730 cm^{-1} and the development of a broad band at 3400 cm^{-1} point out that silanol as well as Brønsted acid sites and/or water molecules from the HPA are consumed. This observation suggests that the HPA

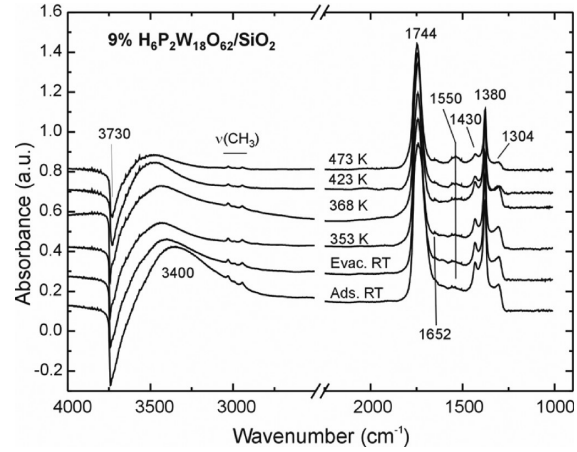

Figure 6. Infrared spectra obtained under *in situ* conditions during the adsorption of gaseous acetic anhydride over 9% $H_6P_2W_{18}O_{62}/SiO_2$ (after calcination at 473 K) from RT to 473 K (Ads., adsorption; Evac., evacuated).

does not cover the whole surface of the silica support, allowing a high exposure of the silanol groups.

It is also worth noting that the intensity of the infrared signals associated with adsorbed silyl ester or acetic acid are now almost 2-fold more intense than that over the bare support. This fact can be interpreted considering that acetic anhydride was hydrolyzed to produce acetic acid more efficiently over the HPA than on pure silica.

An unresolved broad band is now observed at 1550 cm^{-1} due to adsorbed acetate species. Those surface species, molecularly adsorbed acetic acid/silyl ester and acetate, remain adsorbed after heating up to 473 K. Along with those signals, a weak peak was observed at 1652 cm^{-1}, which could be associated with the formation of the acyl intermediate on supported HPA/SiO_2.

3.3. In Situ Investigation of the Surface Interaction of Acetic Anhydride with Supported Wells−Dawson Phosphotungstic Heteropoly Acid in Liquid Media. Further studies of the adsorption and surface reaction of acetic anhydride over the HPA in the liquid media gave more evidence of the presence of a surface acyl intermediate. Figure 7 shows the infrared spectra of liquid acetic anhydride (in carbon tetrachloride medium) in contact with 15% $H_6P_2W_{18}O_{62}/TiO_2$ from room temperature to 317 K. The spectrum of the HPA/TiO_2 in carbon tetrachloride is also shown for comparative purposes.

It is known that the spectra of the phosphotungstic Well−Dawson heteropoly acid possess an intense band at 1075 cm^{-1} assigned to the stretching mode of the P−O bonds [ν(PO)]. This band is considered a fingerprint of the Wells−Dawson heteropolyanion $P_2W_{18}O_{62}^{6-}$ structure.[20] Now, the heteropolyanion in liquid carbon tetrachloride shows the ν(PO) signal at higher wavenumbers than in the gas phase (1086 vs 1075 cm^{-1}). This behavior was reported before by some of us when the influence of various organic substances on the stability of the HPA was investigated.[26] The slight hypsochromic shift of the ν(PO) signal is ascribed to the nondissociative adsorption of organic molecules with low dielectric constant into the cage of tungsten−oxygen species of the heteropolyanion. That interaction is reversible and has no effect on the stability of the structure of the anion.

Molecular acetic anhydride develops the characteristic signals at 1831−1803 and 1761 cm^{-1} assigned to the stretching mode of the carbonyl species [ν(C═O)] along with the signals at 1370 and 1122 cm^{-1} ascribed to the vibrations of methyl and C−O

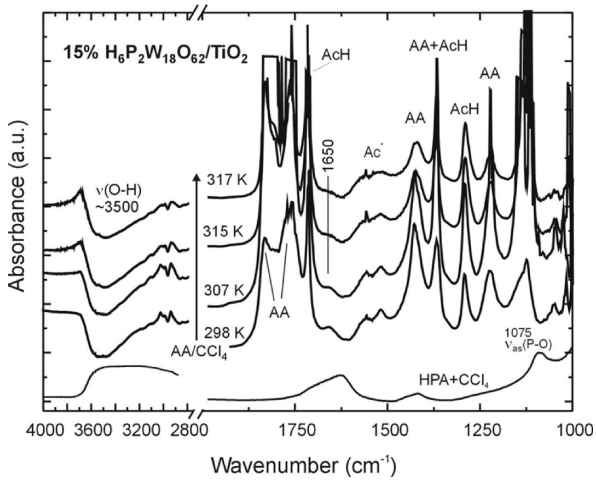

Figure 7. Infrared spectra obtained under *in situ* conditions of the surface adsorbed species on 15% $H_6P_2W_{18}O_{62}/TiO_2$ in contact with an acetic anhydride−CCl_4 mixture (1:10 mol ratio) at various temperatures. (AA, acetic anhydride; AcH, acetic acid, Ac^-, acetate species).

groups.[22] Nevertheless, the ν(C═O) wavenumber of the molecular acetic acid is quite distinctive from that of the anhydride (1715 cm^{-1} of the acid vs 1761 cm^{-1} of the anhydride), which allows a straightforward identification of these two substances.

The intense signal at 1715 cm^{-1} evidences that the acetic anhydride partially decomposes toward acetic acid upon contact with the heteropolyanion at room temperature and that the acid remains in the system up to 317 K. Also, a couple of bands in the 1500−1600 cm^{-1} region developed as the result of the production of acetate species. However, again, a signal of low intensity at 1650 cm^{-1} suggests the presence of another surface species that remains adsorbed up to 315 K. The broad infrared signal belonging to Brønsted acid sites is clearly detected at ∼3500 cm^{-1} without the interference of the organic medium. The suppression of this signal indicates the consumption of the surface acid sites during the adsorption and decomposition processes. Moreover, these sites are not regenerated afterward.

The infrared signal observed at 1650 cm^{-1} upon acetic anhydride adsorption on the HPA, both in gaseous and liquid phase, has been ascribed to the stretching vibration of the acyl species according to previous reports found in the literature. In this context, those previous results on the adsorption and surface decomposition (*in situ* investigations) of various acyl donor species, such as acetic anhydride, acetic acid, and acyl chloride, have been summarized in Table 3. The pioneer investigation of Gorte and co-workers demonstrates the presence of a surface intermediate acyl species on a HZSM-type zeolite upon exposure to either acetic anhydride or acetyl chloride.[27] More recently, Iglesia and co-workers further confirmed the formation of surface acetyl groups on H-zeolites upon exposure to acetic anhydride.[28]

To the knowledge of the authors, there is only one investigation in the open literature based on the interaction of acetic anhydride with a Keggin-type heteropoly acid that was reported by Anderson and co-workers.[16] In that particular case, the infrared stretching vibration of the acyl species was observed at 1654 cm^{-1}, which correlates with our findings.

The observations described in the previous sections about the infrared signals and the surface species observed upon adsorption of acetic anhydride are summarized in Table 4. The comparison of the information obtained in the present investigation with the investigations reported in the literature proves that the acetic anhydride decomposes to acetic acid, acetate, and acyl species over the surface acid sites of the HPA.

Now, a new question arises about the ability of the HPA to further activate the carboxylic acid toward an acyl intermediate species. Therefore, with that idea in mind, the experiment described in Figure 7 was continued by recirculating clean carbon tetrachloride at 321 K for 10 min while the surface species were investigated. The evolution of the surface species presented in Figure 8 shows the characteristic infrared signals of adsorbed acetic anhydride and acetic acid (indicated as AA and AcH, respectively). Clearly, after purging the cell-reactor with pure CCl_4, most of the remaining signals belong to strongly adsorbed acetic acid and acetate groups, and the surface acyl species, previously observed at 1650 cm^{-1}, vanishes after 4 min.

3.3.1. Further Evidence of the Nature of the Active Sites for the Intermediate Acyl Species Genesis over the Heteropoly Acid. The consumption of the Brønsted acid sites observed during the adsorption and decomposition of acetic anhydride over the supported HPA suggests that those species are the active sites of the genesis of the acyl intermediate species (CH_3CO^+). Further evidence of the role of the Brønsted acid sites was obtained through the adsorption of the acyl donor over the zirconia supported HPA previously exchanged with liquid deuterium oxide in the *in situ* cell. Figure 9 shows the infrared spectra of the 14% HPA/ZrO_2 treated with D_2O at 348 K, after in situ drying at the same temperature and under flowing carbon tetrachloride at RT previous to the adsorption of acetic anhydride.

TABLE 3: Summary of the Infrared Signals Reported in the Literature upon Adsorption of Acylating Agents on Various Materials

adsorbate	material	technique	adsorbed species	wavelength	ref
acetic anhydride ($CH_3COOOCH_3$)	$H_3PW_{12}O_{40}/SiO_2$	*in situ* FTIR cell	ν(C═O) phys. ads. dimeric acetic acid	1716, 1403 cm^{-1}	16
			ν(C═O) silyl ester species	1758 cm^{-1}	
			$\delta_s(CH_3)$, $\delta_{as}(CH_3)$	1435, 1384 cm^{-1}	
	$H_3PW_{12}O_{40}/SiO_2ZrO_2$		$\nu_{as}(COO^-)$, $\nu_s(COO^-)$	1550, 1457 cm^{-1}	
			acyl species	1654 cm^{-1}	
			molecular acetic anhydride	1831 cm^{-1}	
acetic acid	H-ZSM-5	*in situ* FTIR cell	ν_{as}(C═O), ν_s(C═O) weakly adsorbed acetic acid	1808, 1790 cm^{-1}	
			acetic acid interacting with Brønsted acid sites	1745 cm^{-1}	27
			acetic acid adsorbed on Brønsted sites	1740, 1750 cm^{-1}	
acetyl chloride (CH_3O-Cl)			ν(C−Cl), ν(C═O) weakly adsorbed acetyl chloride	1900, 1810 cm^{-1}	
			ν(C═O) acetyl-zeolite	1705 cm^{-1}	
acetic anhydride	acidic zeolites	*in situ* FTIR cell	ν(C═O) acetyl	1705, 1755 cm^{-1}	28

TABLE 4: Summary of the Nature of the Adsorbed Species and the Corresponding Infrared Signal of Molecular Acetic Anhydride, Molecular Acetic Acid and Acetic Anhydride Adsorbed over TiO_2, SiO_2, and ZrO_2 Supported Phosphotungstic Wells-Dawson Heteropolyacid Materials and the Corresponding Oxide Supports[a]

acetic anhydride	ν(CO−O−CO) = 1831, 1809 cm^{-1}	ν(C=O) = 1760 cm^{-1}	δ_{as}(CH$_3$) = 1428 cm^{-1}	δ_s(CH$_3$) = 1367 cm^{-1}	ν(C−O) = 1223 cm^{-1}	ν(C−O) = 1114 cm^{-1}	ν(CH$_3$) = 2934 cm^{-1}
acetic acid		ν(C=O) = 1715 cm^{-1}	δ_{as}(CH$_3$) = 1416 cm^{-1}	δ_s(CH$_3$) = 1284 cm^{-1}			ν(CH$_3$) = 3022−2930 cm^{-1}
AA on TiO_2	adsorbed acyl [CH$_3$CO$^+$]	adsorbed acetate (CH$_3$COO−Ti)					
	ν(C=O) = 1675 cm^{-1}	ν_{as}(COO) = 1530 cm^{-1}	ν_s(COO) + δ_{as}(CH$_3$) = 1450 cm^{-1}	δ_s(CH$_3$) = 1340 cm^{-1}			
AA on HPA/TiO_2	adsorbed acetic anhydride [(CH$_3$CO)$_2$O−Ti]	adsorbed acetic acid (CH$_3$COOH−O−Ti)	adsorbed acyl [CH$_3$CO$^+$−O−DW]	adsorbed acetate (CH$_3$COO−Ti)			
	ν(C=O) = 1825 + 1802 cm^{-1}	ν(C=O) = 1750 cm^{-1}	ν(C=O) = 1650 cm^{-1}	ν_{as}(COO) = 1523 cm^{-1}	ν_s(COO) + δ_{as}(CH$_3$) = 1450 cm^{-1}	δ(CH$_3$) = 1294 cm^{-1}	
AA on ZrO_2	adsorbed acetic anhydride [(CH$_3$CO)$_2$O−Zr]	adsorbed acetate (CH$_3$COO−Zr)					
	ν(C=O) = 1830 + 1773 cm^{-1}	ν_{as}(COO) = 1544 cm^{-1}	ν_s(COO) = 1466 cm^{-1}	δ_{as}(CH$_3$) = ∼1400 cm^{-1}	δ_s(CH$_3$) = 1320 cm^{-1}	ν(C−O) = 1131 cm^{-1}	ν(CH$_3$) = 2933 cm^{-1}
AA on HPA/ZrO_2	adsorbed acetic anhydride [(CH$_3$CO)$_2$O−Zr]	acyl [CH$_3$CO$^+$−O−DW]	adsorbed acetate (CH$_3$COO−Zr)				
	ν(C=O) = 1830 + 1803 + 1773 cm^{-1}	ν(C=O) = 1665 cm^{-1}	ν_{as}(COO) = 1530 cm^{-1}	ν_s(COO) = 1451 cm^{-1}	δ_{as}(CH$_3$) = 1396 cm^{-1}	δ_s(CH$_3$) = 1340 cm^{-1}	
AA on SiO_2	adsorbed acetic anhydride [(CH$_3$CO)$_2$O−Si]				adsorbed acetic acid (CH$_3$COOH−O−Si) or silyl ester surface species (CH$_3$CO−O−Si)		
	ν(C=O) = 1827 + 1803 cm^{-1}	δ_{as}(CH$_3$) = 1430 cm^{-1}	δ_s(CH$_3$) = 1373 cm^{-1}		ν(C=O) = 1744 cm^{-1}	ν(COO) + δ(CH$_3$) = 1377 cm^{-1}	δ(CH$_3$) = 1325 cm^{-1}
AA on HPA/SiO_2	adsorbed acetic acid (CH$_3$COOH−O−Si)	acyl [CH$_3$CO$^+$−O−DW]	acetate (CH$_3$COO−Si)				
	ν(C=O) = 1744 cm^{-1}	ν(C=O) = 1652 cm^{-1}	ν_{as}(COO) = 1550 cm^{-1}				
	δ_{as}(CH$_3$) = 1430 cm^{-1}						
	δ_s(CH$_3$) = 1380 cm^{-1}						
	δ(CH) = 1304 cm^{-1}						

[a] HPA, $H_6P_2W_{18}O_{62}$; AA, acetic anhydride.

Figure 8. Infrared spectra obtained under *in situ* conditions of carbon tetrachloride recirculating over 15% $H_6P_2W_{18}O_{62}/TiO_2$ at 321 K up to 10 min (AA, acetic anhydride; AcH, acetic acid; Ac$^-$, acetate species).

Figure 9. Infrared spectra of 14% $H_6P_2W_{18}O_{62}/ZrO_2$ treated with liquid D_2O at 348 K, drying under an argon flow at 348 K and under a carbon tetrachloride flow in the *in situ* cell for experiments in the liquid medium. (**) carbonate species of the ZrO_2 support.

The phosphotungstic Wells−Dawson heteropolyanions, $P_2W_{18}O_{62}^{6-}$, are bonded in the secondary structure by means of H_2O molecules, which forms a network of hydrogen bridge bonds. These bonds between hydrogen linked to terminal oxygen atoms of W═O species and this unit joined to an oxygen of a water molecule, forming the dioxonium structure $H_5O_2^+$ that vibrates in the 3000−3699 cm^{-1} range.[29,30]

The isotopic exchange of hydrated HPA with deuterium oxide can be pictured through the following equations (eqs 1 and 2)

$$D_2O + H_3O^+{-}OW \rightarrow D_2OH^+{-}OW + H_2O \quad (1)$$

$$D_2O + H^+{-}OW \rightarrow D{-}OW + D{-}OH \quad (2)$$

The formation of deuterated D_2OH^+−OW and D−OH species shifts the stretching vibration of the dioxonium $H_5O_2^+$ species (initially centered at 3440 cm^{-1}) toward ∼2500 cm^{-1}, as observed in Figure 9. Similar results were reported by Misono and co-workers in the isotopic exchange of 12-tungstophosphoric acid.[31]

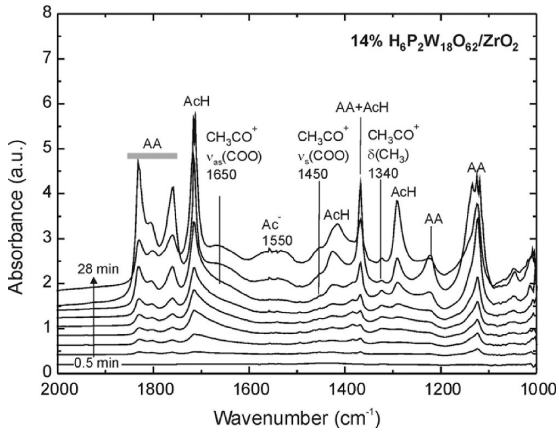

Figure 10. Infrared spectra as a function of time of the adsorption of liquid acetic anhydride (in a 1:10 mol ratio with CCl_4) on 14% $H_6P_2W_{18}O_{62}/ZrO_2$ at 317 K (AA, acetic anhydride; AcH, acetic acid).

Previous investigations also reported two additional bands at 1705 and 1620 cm^{-1} that have been assigned to the bending vibration of the hydroxonium ion H_3O^+ or $H_5O_2^+$ and non-protonated water molecules, respectively.[29,32] Therefore, it is expected that the H−D isotopic exchange of those species shifts their bending vibrations toward lower wavenumbers, as is shown in the following paragraph.

The replacement of the hydrogen atom in the O−H species by a deuterium atom modifies the frequency of the bending vibration band according to the equation $\nu = {}^1/_2\pi(k/\mu)^{1/2}$, where ν stands for the frequency, k stands for the bond force constant, and μ stands for the reduced mass involved in the vibration. Then, the ratio of frequencies for the bending vibrations of the O−H and O−D species results in the following equation:

$$\frac{\bar{\nu}(\mathrm{OH})}{\bar{\nu}(\mathrm{OD})} = \sqrt{\frac{\mu_{\mathrm{OD}}}{\mu_{\mathrm{OH}}}}$$

where $\bar{\nu}$ is the wavenumber (reciprocal of the frequency) and μ_{OH} and μ_{OD} are the reduced masses of the OH and OD species, respectively.

Thus, this wavenumber theoretical ratio is equal to 1.37, which is in agreement with the observed shift of the bending vibration of the O−H species from 1620 to 1194 cm^{-1} (see Figure 9).

The spectroscopic identification of unstable CH_3CO^+ species is based on the generation of the ν(C═O) signal at 1650 cm^{-1}. However, this signal could be perturbed by the δ(OH) of water or dioxonium, $H_5O_2^+$, species in the HPA at 1620 and 1670 cm^{-1}, respectively.[32]

Thus, deuteration of the HPA circumvents the interference of the δ(OH) signals in the 1600−1700 cm^{-1} region. Therefore, new signals emerging in this region can be assigned straightforwardly.

Now, the exchanged HPA/ZrO_2 was contacted with acetic anhydride in the *in situ* cell and their interaction was followed through infrared spectroscopy upon time. Figure 10 shows the evolution of the Brønsted sites along with the acyl species from 0.5 to 28 min of reaction with the acyl donor. It is important to notice that the starting spectrum (deuterated HPA under CCl_4 shown in Figure 9) was subtracted from the subsequent spectra for a direct analysis of the results. Similarly to the results discussed above, the interaction of the acetic anhydride with the deuterated HPA produces acetic acid, adsorbed acetate species, and the intermediate acyl species, as observed in Figure 10. Now it is possible to detect, along with the band ν(C═O) at 1650 cm^{-1}, two additional features at 1450 and 1340 cm^{-1}, which are assigned to ν_s(COO) and $\delta(CH_3)$, respectively, of the CH_3CO^+ species.

4. Discussion

The investigation of the adsorption of acetic anhydride over various oxide based materials through *in situ* infrared spectroscopy provides useful information to understand the genesis of the intermediate acyl species. In this context, the mechanism of interaction of gaseous acetic anhydride with SiO_2, TiO_2 support oxides, and the heteropoly acid is depicted in reactions 3−7.

The decomposition of acetic anhydride toward acetic acid in the presence of traces of water or surface hydroxyls has been detected regardless of the medium (gaseous or liquid) in which the experiments were performed (reaction 3). The acid further reacts with the surface silanol sites of silica and remains strongly adsorbed as a silyl ester or acetic acid (see reactions 4 and 5) in accordance with previous observations of Bachiller-Baeza and Anderson.[16]

$$CH_3CO{-}O{-}COCH_3 + H_2O \rightarrow 2CH_3COOH \quad (3)$$

$$CH_3COOH + Si{-}OH \rightarrow CH_3COO{-}Si + H_2O \quad (4)$$

or

$$CH_3COOH + Si{-}OH \rightarrow CH_3COOH\cdots OH{-}Si \quad (5)$$

The adsorption of acetic anhydride and/or acetic acid over titania generates strongly adsorbed acetate species. In this context, previous reports demonstrated that carboxylic acids dissociatively adsorb on a titania surface at room temperature to form carboxylate groups ($RCOO^-$), and the liberated protons are bound to bridging oxygen atoms forming OH species.[33]

In addition, the work of Asakura and co-workers gives strong evidence of the dissociative chemisorption of acetic anhydride toward acetate and acyl species on a titania surface[33,34] (see reaction 6). Their investigation demonstrated that the dissociative chemisorption of acetic anhydride over TiO_2(110) single crystals generates both acetate (CH_3COO^-) species (adsorbed on 5-fold Ti^{4+} sites) and acyl (CH_3CO^+) species that further react with a surface oxygen, creating more acetate species and an oxygen vacancy (see reactions 7 and 8).

A closer look at the infrared spectra of the adsorption of acetic anhydride over TiO_2 (see Figure 1) shows not only the signals of the symmetric and asymmetric stretching vibration of the acetate species but also another band at 1675 cm^{-1} that might correspond to the surface acyl species. This surface species appears as soon as the anhydride contacts the titania surface at RT and vanishes above 368 K, which can account for its conversion toward acetate species (reaction 8).

$$CH_3CO{-}O{-}COCH_3 + Ti{-}OH \rightarrow CH_3COOH + CH_3CO^+\cdots Ti{-}O^- \quad (6)$$

$$CH_3COOH + Ti{-}OH \rightarrow CH_3COO^- \cdots Ti^{\delta+} + H_2O \quad (7)$$

$$CH_3CO^+ + O_{surf} \rightarrow CH_3COO^- \quad (8)$$

After supporting the HPA on SiO_2, it is clear that the amount of silyl acetate or adsorbed acetic acid notoriously increased as compared to the pure support (see Figures 1 and 2). Also, the formation of acetate species is distinguished at approximately 1550 cm^{-1} together with a very small signal at 1652 cm^{-1} due to the formation of little amounts of acyl species on the HPA/SiO_2. Probably, the low HPA loading on silica (9% w/w) can explain the hard detection of the acyl intermediate on this last catalyst.

The results of the acetic anhydride adsorption on 15% HPA/TiO_2 and 14% HPA/ZrO_2 shown in Figures 2 and 4, containing a higher HPA loading on more basic supports as compared to SiO_2, demonstrate the formation of CH_3CO^+. Furthermore, not only gaseous acetic anhydride chemisorbs dissociatively over oxide-supported Wells−Dawson HPA, generating the acyl intermediate species, but also acetic anhydride in the condensed phase has proved to be able to show the formation of the said intermediate. Additionally, the adsorption of acetic anhydride, both in gaseous and liquid phase, on supported HPA also gives evidence of the role of the Brønsted acid sites of the HPA as the active sites of the adsorption and decomposition of acetic anhydride toward the intermediate acyl species.

Previous investigations demonstrated that the Brønsted acid sites of fully hydrated phosphotungstic heteropoly acid ($H_6P_2W_{18}O_{62}\cdot nH_2O$) are associated with up to 24 molecules of water of crystallization.[29] The HPA suffers a sequential dehydration upon heating through the desorption of 17 mol of water per Wells−Dawson unit between 339 and 345 K, an additional 5 mol of water between 370 and 387 K, and the last two are desorbed in the 581−591 K range. Since the HPA was calcined for 30−60 min at 373−473 K previous to the adsorption experiments described in the present paper, it is possible to ensure that the HPA structure retained the last two molecules of water before the adsorption of the acetic anhydride. The acetic anhydride decomposes toward acetic acid after being in contact with the associated water molecules, leaving the Brønsted acid sites "dehydrated" as pictured in reaction 10. Those sites, free of associated water, are capable of activating the dissociative chemisorption of the anhydride toward the intermediate acyl species (reaction 9).

$$CH_3CO{-}O{-}COCH_3 + H_2OH^+{-}OW \rightarrow 2CH_3COOH + H{-}OW \quad (9)$$

$$CH_3CO{-}O{-}COCH_3 + H{-}OW \rightarrow CH_3CO^+ \cdots OW + CH_3COOH \quad (10)$$

where H−OW stands for a Brønsted acid site of the HPA.

Our results of catalytic measurements have shown the capability of the HPA to catalyze the selective acylation of isobutylbenzene (see Table 2). However, deactivation occurred almost immediately, which prevented the further formation of *p*-isobutylacetophenone.

Most of the literature concerning the heterogeneous Friedel−Crafts acylation or organic substances accounts for the deactivation of the catalytic material during the reaction. Reviewing the literature presented in Table 1 makes it clear that there are few investigations addressing the causes of the deactivation which is informed as a decrease or even null catalytic activity without further explanation.

Nevertheless, Pérot and co-workers investigated the organic substances remaining on the surface of HY and Hβ zeolites after the acylation of 1,2-dimethoxybenzene with acetic anhydride in the liquid phase.[35] The authors attributed the deactivation of the catalysts to di- and triketones and cyclization products irreversibly adsorbed on the zeolites.

More recently, the investigation reported by Apesteguía and Padró demonstrated that the deactivation of several zeolites in the gas phase acylation of phenol with acetic acid is related to a carbonaceous deposit on the surface of the catalysts.[8]

To the knowledge of the authors, the present investigation addresses for the first time in the literature the role of acetate species and acetic acid in the acylation process carried out in the gas and liquid phase over a type of heteropoly acid material.

The dissociative chemisorption of gaseous acetic anhydride and preliminary results of a mixture of isobutylbenzene−acetic anhydride on the HPA show the production of acetate species (in addition to the intermediate reactive acyl species) that remains strongly adsorbed even at temperatures as high as 473 K. Moreover, the formation of acetic acid and its strong adsorption on the HPA could be a serious drawback on the applicability of this material as a catalyst in a Friedel−Crafts acylation in the liquid medium. At this point, two interesting conclusions were obtained: First, the HPA is unable to form the acyl intermediate species from a carboxylic acid like acetic acid. Second, carbon tetrachloride (used as a cosolvent in the liquid medium) is unable to remove the strongly adsorbed acetic acid from the HPA surface. Then, further research should take into account the inhibition of such acetate groups in the genesis of acyl species.

5. Conclusions

The present investigation demonstrates that the phosphotungstic Wells−Dawson heteropoly acid $H_6P_2W_{18}O_{62}\cdot nH_2O$ activates the acetic anhydride to generate an intermediate acyl species in the Friedel−Crafts acylation. Gaseous and liquid acetic anhydride adsorbs and decomposes on the HPA, generating the intermediate acyl species along with acetate species and acetic acid that remains strongly adsorbed. The acetate species observed in the gas phase adsorption are not removed even at 473 K. Moreover, molecular acetic acid adsorbed on the HPA in the liquid media was not removed after recycling of a cosolvent. These observations allow concluding that those species inhibit the catalytic activity and further deactivate the heteropoly acid.

Brønsted acid sites of the heteropoly acid are the active sites of the adsorption-decomposition of the acyl donor substances. The materials investigated are composed by bulk Wells−Dawson HPA that retains at least 2 mol of structural water per Wells−Dawson $P_2W_{18}O_{62}^{6-}$ unit. This partially hydrated state allows the HPA to behave in its pseudoliquid form; therefore, both surface and bulk acid sites might be active in the adsorption of acetic anhydride.

Acknowledgment. The authors acknowledge the financial support of the Agencia Nacional de Promoción Científica y Tecnológica (projects PICT Red 729/06 and PME 311/06) and Universidad Nacional de La Plata (Project 11 X-485).

References and Notes

(1) Friedel, C.; Crafts, J. M. *Comptes Rendus* **1877**, *84*, 1392–1450.
(2) Baddeley, G.; Wrench, E. *J. Chem. Soc.* **1956**, 4943–4945.

(3) Lindley, D. D.; Curtis, T. A.; Ryan, T. R.; de la Garza, E. M.; Hilton, C. B.; Kenesson, T. M. Process for the Production of 4-isobutylacetophenone, USS Patent 05068448 (November 26, 1991).
(4) Chapman, C. J.; Frost, C. G.; Hartley, J. P.; Whittle, A. J. *Tetrahedron Lett.* **2001**, *42*, 773–775.
(5) Arata, K.; Nakamura, H.; Shouji, M. *Appl. Catal.* **2000**, *197*, 213–219.
(6) Jaimol, T.; Pandey, A. K.; Singh, A. P. *J. Mol. Catal. A: Chem.* **2001**, *170*, 117–126.
(7) Kantam, M. L.; Ranganath, K. V. S.; Sateesh, M.; Kumar, K. B. S.; Choudary, B. M. *J. Mol. Catal. A: Chem.* **2005**, *225*, 15–20.
(8) Padró, C. L.; Apesteguía, C. R. *Catal. Today* **2005**, *107*, 258–265.
(9) Izumi, Y.; Ogawa, M.; Urabe, K. *Appl. Catal.* **1995**, *132*, 127–140.
(10) Kaur, J.; Griffin, K.; Harrison, B.; Kozhevnikov, I. V. *J. Catal.* **2002**, *208*, 448–455.
(11) Yadav, G. D.; Manyar, H. G. *Microporous Mesoporous Mater.* **2003**, *63*, 85–96.
(12) Cardoso, L. A. M.; Alves, W., Jr.; Gonzaga, A. R. E.; Aguiar, L. M. G.; Andrade, H. M. C. *J. Mol. Catal. A: Chem* **2004**, *209*, 189–197.
(13) Tagawa, T.; Amemiya, J.; Goto, S. *Appl. Catal.* **2004**, *257*, 19–23.
(14) Yadav, G. D.; Bhagat, R. D. *J. Mol. Catal. A: Chem.* **2005**, *235*, 98–107.
(15) Kozhevnikov, I. V. *Appl. Catal., A* **2003**, *256*, 3–18.
(16) Bachiller-Baeza, B.; Anderson, J. A. *J. Catal.* **2004**, *228*, 225–233.
(17) BHC Company, The Presidential Green Chemistry Challenge Awards Program, Environmental Protection Agency EPA 744-S-97-001, Office of Pollution Prevention and Toxics, Washington, DC, p 1007.
(18) Haggin, J. Catalysis Critical to Benign Process Design. *Chem. Eng. News* **1994**, *72* (April 18), 22–25.
(19) Anastas, P. T.; Bartlett, L. B.; Kirchhoff, M. M.; Williamson, T. C. *Catal. Today* **2000**, *55*, 11–22.
(20) (a) Matkovic, S. R.; Valle, G. M.; Gambaro, L. A.; Briand, L. E. *Catal. Today* **2008**, *133*, 192–199. (b) Matkovic, S. R.; Valle, G. M.; Briand, L. E. *Mater. Res.* **2005**, *8*, 351–355.
(21) Silverstein, R. M.; Bassler, G. C.; Morrill, T. C. *Spectrometric Identification of Organic compounds*; J. Wiley & Sons, Inc.: New York, 1991; pp 91−164.
(22) Bellamy, L. J. *The Infrared Spectra of Complex Molecules*, 3rd ed.; Chapman & Hall: London, 1975.
(23) Rachmady, W.; Vannice, M. A. *J. Catal.* **2002**, *207*, 317–330.
(24) Jackson, S. D.; Kelly, G. J.; Lennon, D. *React. Kinet. Catal. Lett.* **2000**, *70*, 207–212.
(25) Nakamoto, K. *Infrared and Raman Spectra of Inorganic and Coordination Compounds*, 4th ed.; Wiley: New York, 1986.
(26) Valle, G. M.; Briand, L. E. *Mater. Lett.* **2003**, *57*, 3964–3969.
(27) Kresnawahjuesa, O.; Gorte, R. J.; White, D. *J. Mol. Catal. A: Chem.* **2004**, *208*, 175–185.
(28) P. Cheung, P.; Bhan, A.; Sunley, G. J.; Law, D. J.; Iglesia, E. *J. Catal.* **2007**, *245*, 110–123.
(29) Sambeth, J. E.; Baronetti, G. T.; Thomas, H. J. *J. Mol. Catal. A: Chem.* **2003**, *191*, 35–43.
(30) Bielanski, A.; Lubanska, A. *J. Mol. Catal. A: Chem.* **2004**, *224*, 179–187.
(31) Lee, K. Y.; Mizuno, N.; Okuhara, T.; Misono, M. *Bull. Chem. Soc. Jpn.* **1989**, *62*, 1731–1739.
(32) Okuhara, T.; Mizuno, N.; Misono, M. *Adv. Catal.* **1996**, *41*, 113–252.
(33) Ashima, H.; Chun, W.-J.; Asakura, K. *Surf. Sci.* **2007**, *601*, 1822–1830.
(34) Kinoshita, K.; Suzuki, S.; Chun, W.-J.; Takakusagi, S.; Asakura, K. *Surf. Sci.* **2009**, *603*, 552–557.
(35) Guignard, C.; Pédron, V.; Richard, F.; Jacquot, R.; Spagnol, M.; Coustard, J. M.; Pérot, G. *Appl. Catal., A* **2002**, *234*, 79.

JP108031H